Bull Environ Contam Toxicol
DOI 10.1007/s00128-017-2045-2

Design and Development of Acetylthiocholine Electrochemical Biosensor Based on Zinc Oxide–Cerium Oxide Nanohybrid Modified Platinum Electrode

Manju Bhargavi Gumpu[1,2,3] · Noel Nesakumar[1,3,4] · Srinidhi Nagarajan[1,2] · Sadhana Ramanujam[1,2] · Uma Maheswari Krishnan[3,4] · K. Jayanth Babu[1,2] · John Bosco Balaguru Rayappan[1,2,3]

Received: 21 July 2016 / Accepted: 7 February 2017

Abstract Acetylcholinesterase (AChE) enzyme has been predominantly used for the detection of pesticides and metal ions. But, these sensors respond to pesticides as well as metal ions at certain concentration, which results in poor selectivity. Hence in this work, the amount of thiocholine produced during AChE inhibition has been estimated to detect the residual activity of AChE enzyme in-turn to enhance the efficiency of the biosensor. In this context, Pt/ZnO–CeO_2/AChE/Chitosan based biosensor has been developed for sensitive voltammetric quantification of thiocholine in AChE. The sensor exhibited enhanced electron transfer rate, good conductivity and biocompatibility. Both the intrinsic and extrinsic parameters were simultaneously optimized using second order polynomial regression to get the best conditions for ATCh determination. Under optimized experimental conditions, the redox peak current was linear over the concentration range of 0.1–1.5 mM with detection and quantification limit of 0.05 and 0.15 µM respectively and the sensitivity of 1.47 µA mM^{-1}.

Keywords Acetylcholinesterase · Acetylthiocholine · Multivariate optimization · Electrochemical biosensor · Cyclic voltammetry · Nanohybrid

✉ John Bosco Balaguru Rayappan
rjbosco@ece.sastra.edu

[1] Nanosensors Lab, SASTRA University, Thanjavur, Tamil Nadu 613 401, India

[2] School of Electrical & Electronics Engineering, SASTRA University, Thanjavur, Tamil Nadu 613 401, India

[3] Centre for Nanotechnology & Advanced Biomaterials, SASTRA University, Thanjavur, Tamil Nadu 613 401, India

[4] School of Chemical and Biotechnology, SASTRA University, Thanjavur, Tamil Nadu 613 401, India

Hydrolysis of acetylthiocholine (ATCh) by acetylcholinesterase (AChE) enzyme results in the formation of thiocholine. Estimation of thiocholine concentration after AChE inhibition by toxicants (metal ions and pesticides) can be used to investigate the residual activity of AChE (Dan et al. 2013; Pandey et al. 2000; Bucur et al. 2013; Marinov et al. 2010; Er et al. 2014; Pandey & Singh 2011; Mukherjee et al. 2009; Deng & Dong 1996). Since, quantification of thiocholine has potential applications for estimating residual AChE enzyme activity, the detection of thiocholine is of great interest. Several analytical methods have been developed to detect thiocholine such as high performance liquid chromatography, mass spectrometry, fluorescence spectrometry and infrared spectroscopy (Dan et al. 2013; Pandey et al. 2000; Bucur et al. 2013; Marinov et al. 2010; Er et al. 2014; ; Mukherjee et al. 2009; Deng & Dong 1996). Even though these analytical methods are selective and accurate, they require excess reagents and expensive instrumentation (Ramnani et al. 2016; Song et al. 2016; Zhou et al. 2016). In order to overcome these disadvantages, electrochemical biosensors based on AChE enzyme have been used for the selective and sensitive determination of thiocholine. Since the developed electrochemical sensors based on AChE may respond to pesticides and metal ions at certain concentration, they show poor selectivity. Hence in this work, the amount of thiocholine produced during AChE inhibition was investigated to estimate the residual activity of immobilized AChE enzyme. Thus, by estimating the residual AChE enzyme activity after AChE inhibition, the amount of thiocholine produced after AChE inhibition due to toxicants present in groundwater samples can be correlated to the efficiency of toxicants in inhibiting the conversion of ATCh to thiocholine. Prior to the AChE enzyme inhibition, it is important to facilitate good microenvironment for the immobilized AChE enzyme to

Published online: 16 March 2017

retain its catalytic activity. In order to register maximum electrochemical response and to obtain enhanced stability of immobilized AChE enzyme, apart from size variations (Alzahrani et al. 2016; Kozhushner et al. 2014), simultaneous optimization of intrinsic and extrinsic experimental variables is required. Traditionally, multivariate statistical methods have been frequently applied to optimize experimental variables involved in the fabrication of electrochemical biosensor. The main advantages of multivariate statistical methods are to reduce experimental costs and number of experiments, resulting in reduced reagent consumption. Even though multivariate statistical methods are more effective than univariate approaches in finding the optimum conditions for ATCh, the algorithms are too complex. Hence in this work, a second order polynomial model has been developed to analyze and interpret the relation between experimental variables and electrochemical responses. Based on the second order polynomial results, the optimum conditions required for the hydrolysis of ATCh by AChE enzyme has been successfully established. Finally, thiocholine concentrations in AChE in the presence of pesticides and metal ions were determined using multiple linear regression model.

Materials and Methods

For the synthesis of ZnO nanoparticles, zinc acetate and sodium hydroxide were used. An amount of 0.4 mM of zinc acetate was dissolved in deionized water and 0.1 M of sodium hydroxide solution was added drop-wise into zinc acetate solution until the pH reached 11.5. The mixture was vigorously stirred at 333 K for 30 min. Later, the solution was transferred to muffle furnace and annealed at 673 K for 4 h. Finally, the ZnO powder sample was washed with distilled water and dried at 323 K for 6 h. Similarly for the synthesis of CeO_2 nanoparticles, 0.6 mM of cerium acetate was prepared. Then 0.3 M of sodium hydroxide was added gradually while stirring until the pH reached 10.5. The resulting mixture was stirred at 323 K for 3 h. After stirring for 3 h, the solution was annealed at 623 K for 5 h. Finally the powder sample was washed thoroughly with deionized water. Subsequently, the sample was dried in hot air over at 323 K overnight.

In order to prepare ZnO–CeO_2/AChE/Chitosan nanocomposite, different weight percent of ZnO (0.05–0.5 wt%), CeO_2 (0.05–0.5 wt%) and chitosan (0.05–0.5 wt%) was dispersed in AChE solution (50–500 U mL^{-1}) and sonicated for 2 min. Finally, 5 µL of this product was taken and coated onto the Pt electrode's surface. The prepared Pt/ZnO–CeO_2/AChE/Chitosan bioelectrode was washed consecutively with PBS (0.1 M, pH 7.4). The experimental variables (intrinsic and extrinsic variables) which have significant effect on the electrochemical response were simultaneously optimized using first order derivative of second order polynomial model. At each point of the optimized valve (x = a), the tangent to the peak current response curve is parallel to experimental variables (x-axis), i.e., its slope ($= dI_p/dx$, where x is the experimental variable) is zero. It is important to note that $I_p(x)$ is maximum at x = a only if f'(a) is equal to zero and f' (a) is negative [i.e., f'(a) changes sign from positive to negative].

Groundwater collected from local area (Thanjavur) was used to evaluate the analytical performance of the calibrated linear model. At higher ATCh concentration ([ATCh] > [K_M]), the rate of catalytic reaction attains maximum and depends on AChE enzyme activity. In order to estimate the activity of AChE enzyme in contaminated groundwater samples, 1.5 mM ATCh, which was greater than K_M, was added to 10 nM of toxicants namely captan, monocrotophos, dichlorvos, 2,3,7,8-tetrachlorodibenzodioxin, arsenic and cadmium in contaminated groundwater samples. In all cases, the determination of ATCh was performed using cyclic voltammetry scanned over the range of −0.1–0.5 V (*vs Ag/AgCl*). In addition, residual AChE enzyme activity was assessed indirectly by estimating the amount of ATCh involved in the electrocatalytic reaction after AChE inhibition. All cyclic voltammetric measurements were performed under the optimized experimental condition with five-time measurements .

Results and Discussion

The FE-SEM images of ZnO, CeO_2 and ZnO–CeO_2 nanoparticles are shown in Fig. 1A–D. FE-SEM study revealed the formation of sphere and rod like morphologies of CeO_2 and ZnO samples respectively. Large clusters of ZnO and CeO_2 with rod and sphere like morphologies were observed in ZnO–CeO_2 nanocomposites. In order to study the distributions of ZnO, CeO_2 and ZnO–CeO_2 nanoparticles on the working electrode, FE-TEM images (Fig. 1E–J) of ZnO, CeO_2 and ZnO–CeO_2 were recorded. FE-TEM images (Fig. 1E–J) further demonstrated the size distribution of ZnO, CeO_2 and ZnO–CeO_2 nanoparticles on Pt electrode as 6.21 ± 1.24, 5.59 ± 0.88 and 6.04 ± 1.43 nm, respectively. The ZnO, CeO_2 and ZnO–CeO_2 nanoparticles size distributions were positively skewed with values of 0.37, 0.09 and 1.06 respectively. The kurtosis values of ZnO, CeO_2 and ZnO–CeO_2 nanoparticles size distributions were 0.63, −0.19 and 1.30 respectively, demonstrating that the ZnO, CeO_2 and ZnO–CeO_2 nanoparticle size distribution curves would be platykurtic. It also depicted that the number of ZnO, CeO_2 and ZnO–CeO_2 nanoparticles around 6.21 ± 1.24, 5.59 ± 0.88 and 6.04 ± 1.43 nm respectively.

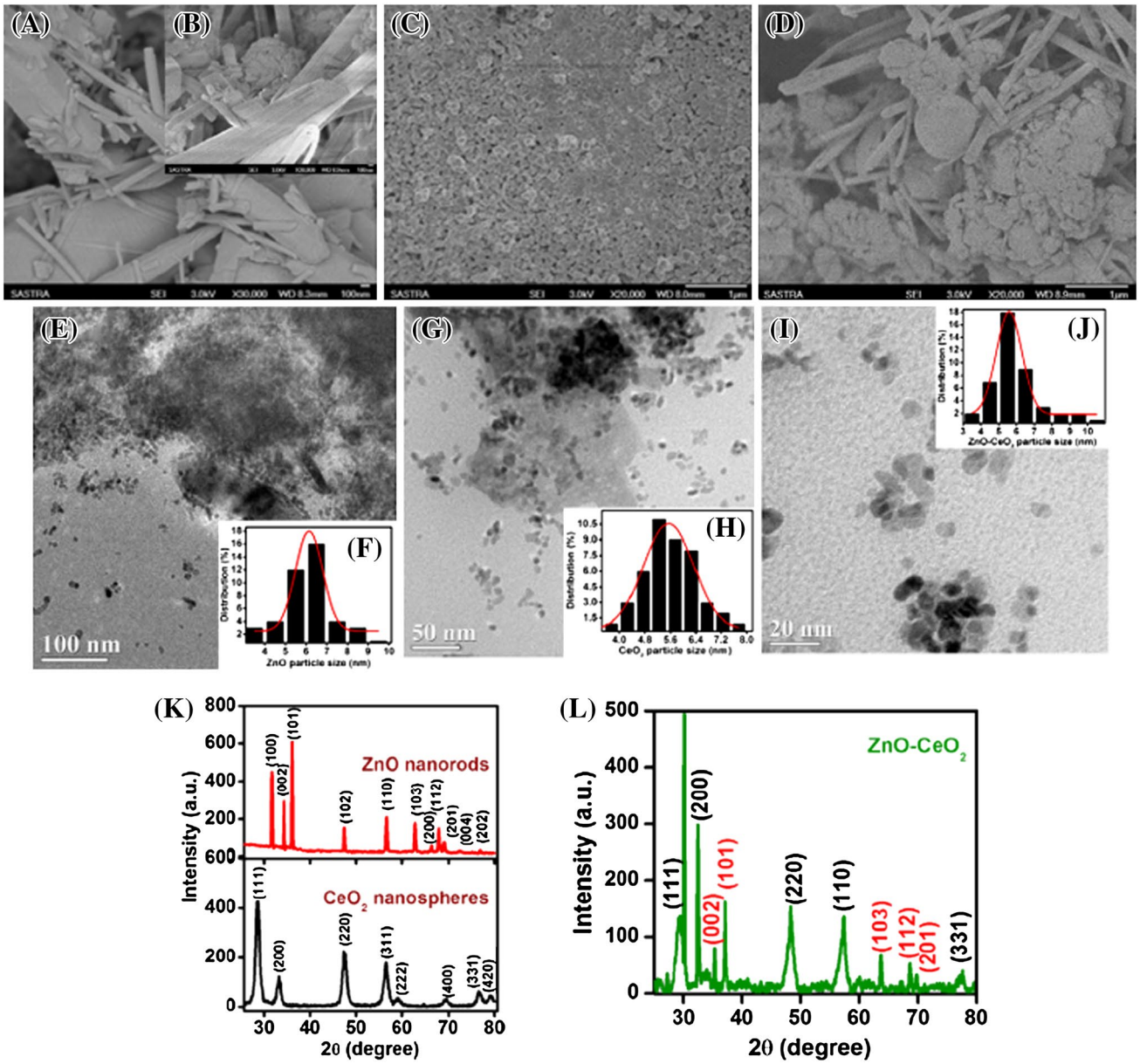

Fig. 1 FE-SEM images of **A**, **B** ZnO, **C** CeO_2 and **D** ZnO–CeO_2, FE-TEM images of **E** ZnO, **F** particle size distribution of ZnO, **G** FE-TEM image CeO_2, **H** particle size distribution of ZnO, **I** FE-TEM image ZnO–CeO_2, **J** particle size distribution of ZnO–CeO_2, **K** XRD patterns of ZnO and CeO_2 nanoparticles, **L** XRD pattern of ZnO–CeO_2

Figure 1K shows the typical XRD patterns of CeO_2 and ZnO nanoparticles. For the as-prepared ZnO nanorods, the detected peaks noticed at 31.59°, 34.13°, 36.09°, 47.44°, 56.47°, 62.74°, 66.26°, 68.02°, 69.40°, 72.54° and 76.90 can be ascribed to the (100), (002), (101), (102), (110), (103), (200), (112), (201), (004) and (202) planes of ZnO according to Joint Committee on Powder Diffraction Standards (JCPDS) card 36-1651. For the as-prepared CeO_2 nanospheres, the diffraction peaks at 28.85°, 32.96°, 47.46°, 56.27°, 59.21°, 69.24°, 76.64° and 79.19° can be assigned to the planes (111), (200), (220), (311), (222), (400), (331) and (420) of CeO_2 (JCPDS card 34-0394). These peaks have confirmed the polycrystalline nature of CeO_2 and ZnO nanoparticles with cubic fluorite and hexagonal wurtzite structures respectively. CeO_2–ZnO nanohybrid exhibited peaks corresponding to both CeO_2 and ZnO signifying that the formed CeO_2–ZnO nanoparticles are polycrystalline in nature (Fig. 1L).

In the absence of AChE enzyme, bare Pt electrode showed flat and featureless voltammograms with relatively small magnitude of current, indicating that there was no redox activity in the applied potential range. On

the contrary, a pair of redox peaks appeared at Pt/AChE/Chitosan, Pt/ZnO/AChE/Chitosan, Pt/CeO_2/AChE/Chitosan and Pt/ZnO-CeO_2/AChE/Chitosan, which showed the direct electron transfer of adsorbed thiocholine on the AChE modified Pt electrodes (Fig. 2A). The observed voltammetric response of the immobilized AChE was ascribed to the electron exchange between adsorbed thiocholine and Pt electrode surface, as described by Eq. (1)

$$\begin{aligned} &Acetylthiocholine\ chloride + H_2O \xrightarrow{AChE} Thiocholine \\ &\quad + Acetic\ acid + Cl^- \\ &2Thiocholine \xrightarrow{Anodic\ potential} Dithio-bis-choline + 2H^+ + 2e^- \\ &Dithio-bis-choline + 2H^+ + 2e^- \xrightarrow{Cathodic\ potential} 2Thiocholine \end{aligned} \quad (1)$$

When ATCh was added to the PBS solution, hydrolysis of ATCh by immobilized AChE enzyme took place, which resulted in the formation of thiocholine before the cyclic voltammetric measurement. At anodic peak potential, AChE modified Pt electrodes oxidized thiocholine to dithio-bis-choline, which was then subjected to cathodic reduction. At cathodic peak potential, dithio-*bis*-choline got reduced to form thiocholine resulting in an effective electron transfer in the AChE modified Pt electrodes. The observed redox potentials of different modified Pt electrodes were in good agreement with the previously reported potential of AChE modified Pt/ZnO and Pt/CeO_2 bioelectrodes suggesting that the observed redox potential was the characteristic redox potential of thiocholine(ox)/thiocholine(red) couple (Table 1).

The redox currents in Pt/ZnO–CeO_2/AChE/Chitosan were approximately 25 and 50% larger than those in Pt/ZnO/AChE/Chitosan and Pt/CeO_2/AChE/Chitosan respectively, indicating that ZnO–CeO_2 nanohybrid had facilitated the direct electron transfer between adsorbed thiocholine and Pt electrode surface. The current enhancement could be ascribed to the excellent electrical conductivity and synergic effect of ZnO and CeO_2 nanoparticles in ZnO–CeO_2 nanohybrid. Owing to numerous Ce–O–Zn linkages between ZnO and CeO_2 nanoparticles, large oxygen storage capacity and oxygen vacancy defects of CeO_2 nanospheres and basic (O^{2-}) and acidic (Zn^{2+}) surface sites of ZnO nanorods, ZnO–CeO_2 nanocomposites enhanced the electrical conductivity between adsorbed thiocholine and Pt electrode (Xie et al. 2013). The formal potential of Pt/ZnO–CeO_2/AChE/Chitosan electrode was 194.5 mV (*vs. Ag/AgCl*), which was similar to that obtained at other AChE enzyme modified Pt electrodes (Table 1). These results demonstrated that ZnO nanorods, CeO_2 nanospheres and ZnO–CeO_2 nanohybrid improved the contact between Pt electrode and immobilized AChE enzyme. The electron transfer rate constant ($K_s = I_p/Q$) of AChE enzyme immobilized on ZnO–CeO_2 nanohybrid in the cathodic and anodic process was estimated as 9.45 and 9.12 s^{-1}, which was higher than the values obtained for AChE enzyme immobilized on ZnO nanorods and CeO_2 nanospheres modified Pt electrodes. This signifies that the ZnO–CeO_2 nanohybrid showed an enhanced electron transfer rate during the electrochemical process (Table 1).

The surface coverage of adsorbed electroactive thiocholine biomolecule on various modified Pt electrodes was estimated. The values of surface coverage of electroactive thiocholine on Pt/ZnO–CeO_2/AChE/Chitosan electrode surface were estimated to be 9.45×10^{-12} mol cm^{-2} (in the cathodic process) and 9.12×10^{-12} mol cm^{-2} (in the anodic process). Comparing these surface coverage values with those obtained for electroactive thiocholine on other immobilization matrices (Table 1), the ZnO–CeO_2 nanomatrix was more effective for thiocholine adsorption. Based on the enhanced surface coverage, biocompatibility, high electron transfer rate and excellent conductivity, Pt/ZnO-CeO_2/AChE/Chitosan electrode was selected for ATCh detection in all further electrochemical studies.

The effect of scan rate (0.1–0.2 Vs^{-1}) on the electrochemical response of Pt/ZnO–CeO_2/AChE/Chitosan electrode is shown in Fig. 2B. From the Fig. 2C, D, it was found that the redox peak potential and current are dependent on the scan rate. The cathodic and anodic peak current increased linearly with scan rate from 0.1 to 0.2 Vs^{-1}. Their corresponding linear regression equations can be expressed as $I_{pc} = 25.52\ [\nu] + 7.26$ ($R^2 = 0.99$) and $I_{pa} = -26.23\ [\nu] - 6.74$ ($R^2 = 0.99$) respectively. These results confirmed that electroactive thiocholine

Table 1 Electrochemical parameters estimated from the cyclic voltammograms of different modified Pt electrodes in 0.1 mM PBS (pH 7.4) containing 0.1 µM of ATCh performed at 0.1 Vs^{-1}

Electrode	I_p (µA)		E_p (V)		ΔE_p (V)	FWHM (V)		K_s (s^{-1})		Γ($\times 10^{-12}$M cm^{-2})	
	Cathode	Anode	Cathode	Anode		Cathode	Anode	Cathode	Anode	Cathode	Anode
Pt/AChE	6.79	6.34	0.154	0.235	0.081	194	187	0.37	0.25	7.12	6.56
Pt/CeO_2/AChE	7.67	7.11	0.154	0.235	0.081	189	180	0.52	0.41	7.95	7.65
Pt/ZnO/AChE	8.42	7.85	0.154	0.235	0.081	189	180	0.76	0.64	8.36	8.21
Pt/ZnO–CeO_2/AChE	9.32	8.61	0.154	0.235	0.081	187	177	1.12	0.84	9.45	9.12

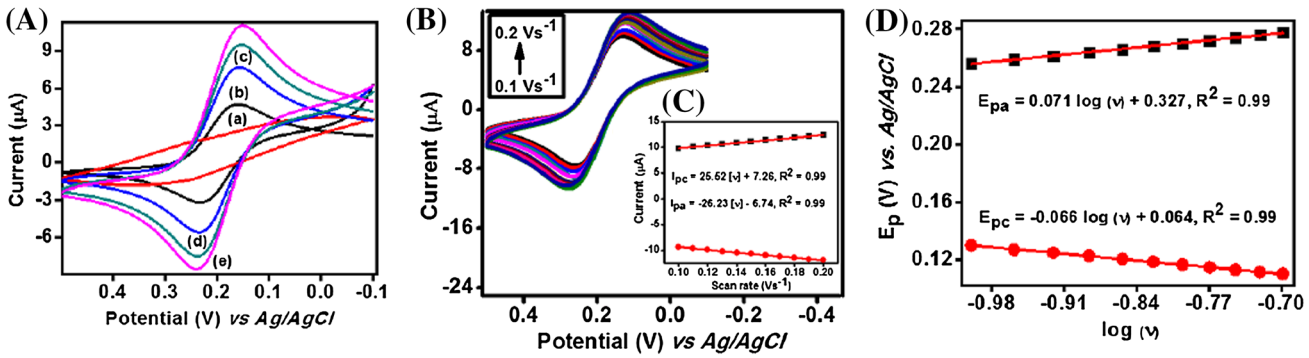

Fig. 2 **A** Effect of different modified electrodes: *a* bare Pt, *b* Pt/AChE/Chitosan, *c* Pt/CeO_2/AChE/Chitosan, *d* Pt/ZnO/AChE/Chitosan and Pt/ZnO–CeO_2/AChE/Chitosan in 0.1 mM PBS (pH 7.4) containing 0.1 µM of ATCh performed at 0.1 Vs^{-1}, **B** effect of varying scan rate (0.1–0.2 Vs^{-1}) on Pt/ZnO–CeO_2/AChE/Chitosan modified electrode in 0.1 mM PBS (pH 7.4) containing 0.1 µM of ATCh, **C** linear dependence of anodic and cathodic peak currents *vs.* scan rate and **D** linear plot of Pt/ZnO–CeO_2/AChE/Chitosan

biomolecule adsorbed onto the Pt/ZnO-CeO_2/AChE/Chitosan electrode surface had undergone a surface confined electron transfer. In order to register maximum peak current response, intrinsic and extrinsic experimental parameters were simultaneously optimized (Figs. 3, 4). For these reasons, second order polynomial equation has been constructed to optimize experimental conditions for ATCh measurement. The general equation is

$$I_p = \beta_0 + \beta_1 x_1 + \beta_2 x_2^2 \quad (2)$$

where x is the experimental variable and β_0, β_1 & β_2 are regression coefficients. Based on the experimental results, regression coefficients were calculated and given in Table 2. The fitted second order polynomial regression model depicted $R^2 = 0.99$, indicating that the fitting happened very well and only 1% of total variance was not explained by these models. The electrochemical response described by Eq. (2) showed a maximum point at an optimized experimental condition can be calculated using the first order derivative of second order polynomial model.

$$\frac{\partial I_p}{\partial x} = 0 \quad (3)$$

By solving Eq. (3), the optimized values for AChE enzyme loading, wt% of ZnO, CeO_2 and chitosan; pH, incubation time and concentration of PBS were found to be 351.435 U mL^{-1}, 0.352 wt%, 0.198 wt%, 0.352 wt%, 7.0 pH, 31.6 min and 0.366 mM respectively (Table 2). It was found that maximum electrochemical response was registered when the experiment was performed under optimized conditions of AChE enzyme loading, wt% of ZnO, CeO_2 and chitosan, pH, incubation time and concentration of PBS. Based on the multivariate analysis, the optimized intrinsic and extrinsic experimental parameters were selected for further electrochemical experiments. Cyclic voltammograms of Pt/ZnO–CeO_2/AChE/Chitosan bioelectrode (Fig. 5A) in the presence of increasing concentrations of ATCh performed at 0.1 Vs^{-1}. It was clearly observed that reduction and oxidation peak current gradually increased with increase in ATCh concentration, which was attributed to the enhanced electron transfer rate between adsorbed thiocholine and Pt electrode by ZnO–CeO_2 nanohybrid. This result showed that the Pt/ZnO–CeO_2/AChE/Chitosan had excellent electrocatalytic behaviour towards ATCh. A calibration plot based on the cathodic and anodic peak currents versus ATCh concentration is presented in Fig. 5B and this plot can be represented by Eq. (4).

$$I_{pc}(\mu A) = 1.47[ATCh]\left(\mu A\ mM^{-1}\right) + 9.74,\ R^2 = 0.99$$

$$I_{pa}(\mu A) = 2.13[ATCh]\left(\mu A\ mM^{-1}\right) + 8.67,\ R^2 = 0.99 \quad (4)$$

Based on these equations, cathodic and anodic sensitivity of 1.47 and 2.13 µA mM^{-1} with a linear range between 0.1 and 1.5 mM was achieved with a correlation coefficient of 0.99. These results could be ascribed to the enhanced electroactive area provided by ZnO–CeO_2 nanohybrid on the Pt electrode surface for AChE enzyme immobilization. The achieved detection (taken as 3.3σ/S, where σ is the standard deviation of the blank signal and S is the sensitivity) and quantification limits (taken as 10σ/S) were 0.05 and 0.15 µM respectively. The maximum current (I_{max}) and Michaelis–Menten constant (K_M) estimated from Lineweaver–Burk plot were calculated to be 13.24 µA and 0.75 mM respectively. The low K_M value indicated a high affinity of immobilized AChE enzyme for its substrate ATCh. A 8×6 matrix was constructed and principal component analysis was employed to discriminate electrochemical parameters. In the cathodic process, Q, E_{pc} and

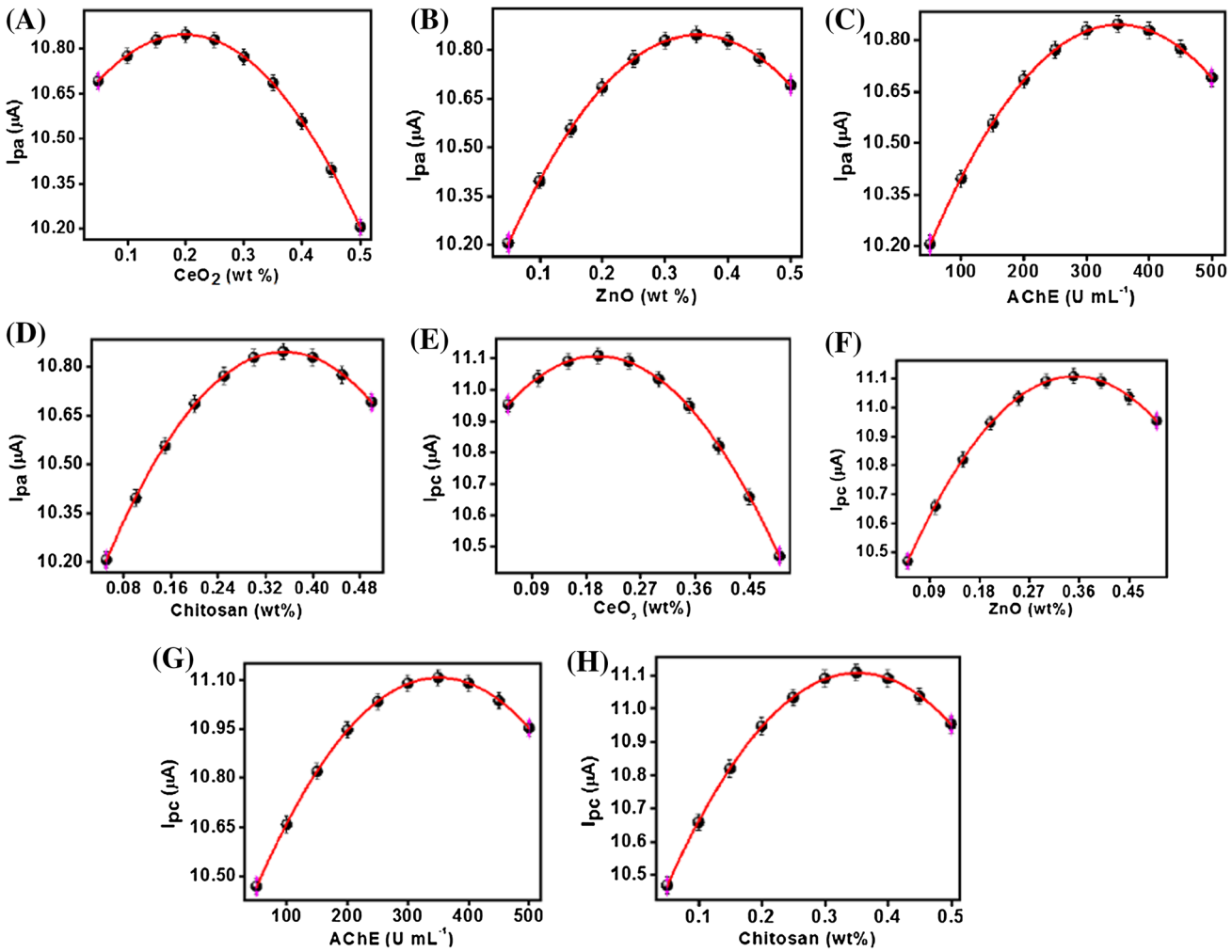

Fig. 3 Effect of CeO_2 **A** and **E** ZnO **B** and **F**, AChE loading **C** and **G** and chitosan **D** and **H** on the cathodic and anodic response of Pt/ZnO–CeO_2/AChE/Chitosan bioelectrode in 0.1 mM PBS (pH 7.4) containing 0.1 µM of ATCh performed at 0.1 Vs^{-1}

FWHM fall in the boundary of upper left, upper right and lower left quadrants, whereas K_s, Γ and I_{pc} fall in the lower left quadrant (Fig. 5C). Even though K_s, Γ and I_{pc} fall in the lower left quadrant, they can be distinguished easily owing to the small distance between two electrochemical parameters within the lower left quadrant. Similarly in the anodic process, I_{pa} & K_s, E_{pa}, FWHM and Γ & Q fall in the boundary of upper left, upper right, lower right and lower left quadrants (Fig. 5D). The distance between I_{pa} & K_s and Γ & Q in the upper and lower left quadrants was large, indicating that PCA can discriminate I_{pa}, K_s, Γ and Q quantitatively. Thus, PCA was used successfully to distinguish the electrochemical parameters involved both in the cathodic and anodic process. In addition, multiple linear regression equations based on FWHM, E_{pc}, E_{pa}, I_{pc}, I_{pa}, Ks, Γ and Q were formulated to estimate ATCh from the cathodic (Eq. (5)) and anodic process (Eq. (6)).

$$[ATCh](mM) = 0.263\left[I_{pc}\right](\mu A) - 9.330 \times 10^{10}[Q](\mu C) - 3.253 \times 10^{-2}\left[E_{pc}\right](mV) + 8.167 \times 10^{-2}[FWHM](mV) \quad (5)$$

$$[ATCh](mM) = 0.453\left[I_{pa}\right](\mu A) - 3.187 \times 10^{12}[Q](\mu C) + 1.809 \times 10^{-2}\left[E_{pa}\right](mV) + 8.314 \times 10^{-2}[FWHM]\,(mV) - 6.91610^{-2}\left[K_s\right]\left(s^{-1}\right) + 1.931 \times 10^{13}[\Gamma](\times 10^{-9} M\ cm^{-2}) - 25.809 \quad (6)$$

In order to investigate the accuracy of the Pt/ZnO–CeO_2/AChE/Chitosan electrode, correlation between added and predicted concentrations of ATCh was calculated (Fig. 5E). An acceptable correlation coefficient of 0.99 with linear regression equation being Predicted [ATCh] (mM) = 1.0 Added [ATCh] (mM) − 0.017 (in cathodic process) and Predicted [ATCh] (mM) = 1.0

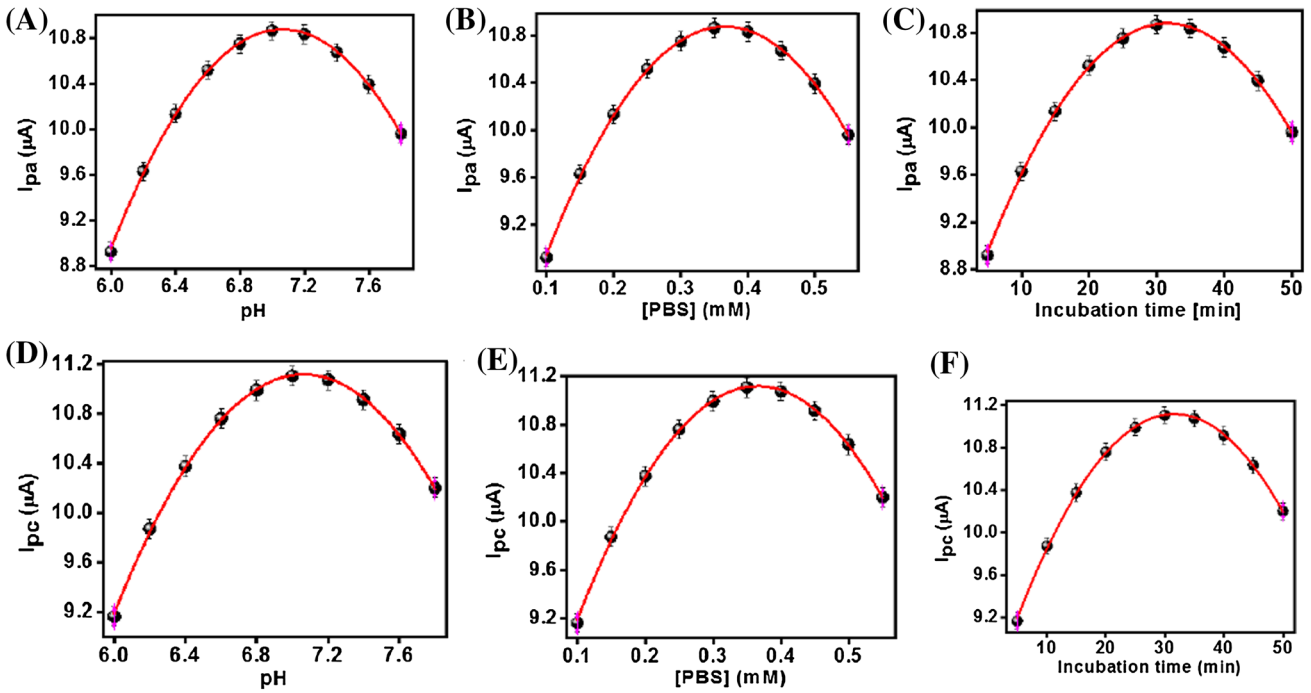

Fig. 4 Effect of pH **A** and **D**, incubation time **E** and **F**, concentration of PBS **B** and **E** on the cathodic and anodic response of Pt/0.352 wt% of ZnO −0.198 wt% of CeO_2/ 351.435 U mL^{-1} of AChE/0.352 wt% of Chitosan bioelectrode containing 0.1 µM of ATCh performed at 0.1 Vs^{-1}

Table 2 Parameters of second order polynomial regression models for the determination of optimized CeO_2, ZnO, AChE loading, chitosan, pH, incubation time and concentration of PBS

Model	β_2	β_1	β_0	R^2	Optimized variable
I_{pa} vs. CeO_2	−7.042	2.795	10.567	0.99	0.198 wt%
I_{pa} vs. ZnO	−7.042	4.952	9.974	0.99	0.352 wt%
I_{pa} vs. AChE	-7.043×10^{-6}	4.95×10^{-3}	9.974	0.99	351.435 U mL^{-1}
I_{pa} vs. Chitosan	−7.042	4.952	9.974	0.99	0.352 wt%
I_{pc} vs. CeO_2	−7.043	2.795	10.830	0.99	0.198 wt%
I_{pc} vs. ZnO	−7.043	4.952	10.236	0.99	0.352 wt%
I_{pc} vs. AChE	-7.043×10^{-6}	4.95×10^{-3}	10.236	0.99	351.435 U mL^{-1}
I_{pc} vs. Chitosan	−7.043	4.952	10.236	0.99	0.352 wt%
I_{pa} vs. pH	−1.706	24.105	−74.260	0.99	7.064 pH
I_{pa} vs. Incubation time	-2.73×10^{-3}	0.172	8.152	0.99	31.600 min
I_{pa} vs. [PBS]	−27.299	19.983	7.221	0.99	0.366 mM
I_{pc} vs. pH	−1.706	24.105	−74.019	0.99	7.064 pH
I_{pc} vs. Incubation time	-2.73×10^{-3}	0.172	8.393	0.99	31.600 min
I_{pc} vs. [PBS]	−27.299	19.983	7.462	0.99	0.366 mM

Added [ATCh] (mM)-3.853×10^{-4} (in anodic process), depicting the satisfactory accuracy of the proposed multiple linear regression equation. It can be seen that multiple linear regression model estimated from the cathodic process gave small RPE (0.304%) and RMSECV (0.280%) with 99.931% recovery whereas, multiple linear regression model estimated from the anodic process showed large RMSECV (1.184%) and poor RPE (1.293%) and recovery (95.736%). These results demonstrated that the proposed multiple linear regression model estimated from the cathodic process was reliable for the determination of ATCh in the presence of pesticide.

The fabricated Pt/ZnO–CeO_2/AChE/Chitosan electrode achieved satisfactory reproducibility and repeatability with the RSD of 1.52 and 1.04% respectively. The Pt/ZnO–CeO_2/AChE/Chitosan electrode retained 96% of its original current response over a period of 20 days. The enhanced stability can be ascribed to the biocompatible microenvironment facilitated by ZnO–CeO_2 nanohybrid around the immobilized AChE enzyme.

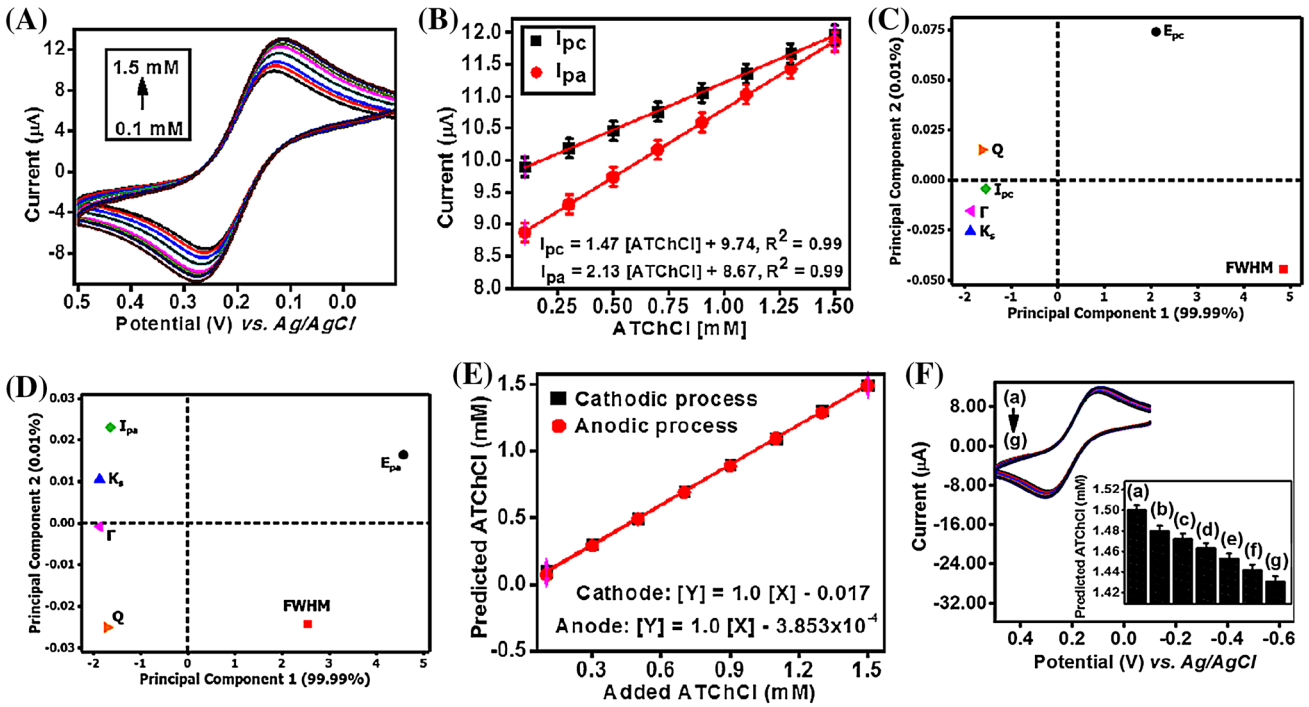

Fig. 5 **A** Cyclic voltammograms of Pt/ZnO–CeO_2/AChE/Chitosan bioelectrode in the presence of increasing concentrations of ATCh performed at 0.1 Vs^{-1}, **B** calibration curves of cathodic and anodic current with ATCh concentration, **C** and **D** principal component analysis of the electrochemical parameters estimated from the cathodic and anodic process for various concentrations of ATCh, **E** correlation between predicted [ATCh] vs. added [ATCh] and **F** cyclic voltammograms obtained from the Pt/ZnO–CeO_2/AChE/Chitosan in PBS (7.064 pH, 0.366 mM) containing 1.5 mM ATCh: *a* ATCh biosensor without pesticide treatment and ATCh biosensor after treatment with *b* 10 nM of captan, *c* monocrotophos, *d* dichlorvos, *e* 2,3,7,8-tetrachlorodibenzodioxin, *f* arsenic and *g* cadmium

Optimization technique of the proposed ATCh biosensor was compared with the other reported ATCh biosensors (Table 3). When compared with the other proposed second order and quadratic polynomial models, only the proposed second order polynomial models showed best results in R^2 (i.e., $R^2 = 0.99$), simplicity and accuracy (Marinov et al. 2010; Bahman et al. 2011; Ebrahimi et al. 2010; Ivanov et al. 2010; Quirós et al. 2014). When compared with multiple linear regression method developed by Ramachandra et al. (Ramachandra et al. 2015), only the presently proposed AChE biosensors with multiple linear regression based chemometric method can effectively enhance the

Table 3 Comparison of optimization technique of the proposed ATCh biosensor with other reported ATCh biosensors

Parameters in experimental design	Polynomial regression	R^2	Optimization technique	Comments	Reference
AChE:MWCNT:acidic sol–gel	Second-order	0.92	Central composite design	Complex algorithm, inaccuracy	Bahman et al. (2011)
AChE:MWCNT	Quadratic	0.89	Response surface methodology	Complex algorithm, inaccuracy	Ebrahimi et al. (2010)
AChE:Concanavalin:MWCNT	Quadratic	0.98	Central composite design	Complex algorithm, accuracy	Ivanov et al. (2010)
AChE:Nano-Au:Bovine serum albumin:Glutaraldehyde	-	0.99	Manual	Complex algorithm, good accuracy and reagent consumption	Marinov et al. (2010)
Applied potential:pH:ATCh	-	-	Central composite design	Complex algorithm, inaccuracy, noisy	Quirós et al. (2014)
ZnO:CeO_2:AChE:Chitosan & pH:[PBS]:Incubation time	Second-order	0.99	Local maximum using first order derivative	Simple algorithm, good accuracy	Present work

Table 4 Comparison of analytical performances of various ATCh biosensors with the developed ATCh biosensor

Nanomaterial	LOD (μM)	Linearity (μM)	Parameter optimization	Reference
MWCNT	0.10	2–400	Univariate	Dan et al. (2013)
Organically modified sol–gel glass	-	-	Univariate	Pandey et al. (2000)
MWCNT	1	-	Univariate	Bucur et al. (2013)
Nano-Au	1.80	10–170	Multivariate	Marinov et al. (2010)
Cobalt Phthalocyanine	-	225–900	Univariate	Er et al. (2014)
PANI–TCNQ–Pd	-	50–10000	Univariate	Pandey & Singh (2011)
Pyrroloquinoline quinine	0.5	0.5–50	Univariate	Mukherjee et al. (2009)
Cobalt Tetraphenyl porphyrin	0.8	5–800	Univariate	Deng & Dong (1996)
$ZnO–CeO_2$	0.05	100–1500	Multivariate	Present work

specificity towards ACh/ATCh owing to its enhanced accuracy and 6 parameter dependence. The analytical performance of Pt/$ZnO–CeO_2$/AChE/Chitosan was compared to that of other reported of ATCh biosensors (Table 4). Owing to the combined fast electron transfer and biocompatible properties of ZnO and CeO_2 nano-interfaces, the developed sensor detected ATCh in concentrations down to 0.05 μM, which was lower than the detection limits reported for previously reported ATCh sensors based on multi- and univariate optimization.

Cyclic voltammetric behaviour (Fig. 5F) of Pt/$ZnO–CeO_2$/AChE/Chitosan electrode after treatment with 10 nM of toxicants namely captan, monocrotophos, dichlorvos, 2,3,7,8-tetrachlorodibenzodioxin, arsenic and cadmium in groundwater containing 1.5 mM ATCh. The redox peak current obtained in the presence of pesticide was much lesser than that in the absence of ATCh. The degree of AChE inhibition by toxicants was in the order of captan > monocrotophos > dichlorvos > 2,3,7,8-tetrachlorodibenzodioxin > arsenic > cadmium. The decrease in redox peak current was due to stronger interaction between pesticide and serine hydroxyl group of AChE enzyme. Thus the catalytic activity of immobilized AChE enzyme got affected and less thiocholine was released per second, giving a lower redox current response. The detected ATCh in the presence of captan, monocrotophos, dichlorvos, 2,3,7,8-tetrachlorodibenzodioxin, arsenic and cadmium were 1.48, 1.472, 1.463, 1.453, 1.442 and 1.431 mM respectively. In order to check the significant difference between the current response of ATCh biosensor without toxicant treatment and ATCh biosensor with toxicant treatment, student's paired *t*-test at 95% confidence interval was performed. It was found that there was a significant difference between the current response of ATCh biosensor without toxicant treatment and ATCh biosensor with toxicant treatment ($p < 0.05$). These results clearly indicated the inhibition of AChE enzyme activity by tested toxicants. As a result, the redox peak current response to ATCh can be employed to monitor toxicity of contaminants to immobilized AChE and gave a simple way of investigating the effect of toxicants on the immobilized AChE enzyme.

A highly sensitive cyclic voltammetric thiocholine biosensor was successfully fabricated by immobilizing AChE on $ZnO–CeO_2$ nanohybrid modified Pt electrode. The $ZnO–CeO_2$ nanohybrid efficiently enhanced the electron transfer between the adsorbed thiocholine and Pt electrode surface due to the excellent synergy effect of $ZnO–CeO_2$ nanohybrid. In addition, computational analysis was performed on intrinsic and extrinsic electrochemical parameters with the purpose to find out the best experimental conditions for running cyclic voltammetry on ATCh solution. Classification of electrochemical parameters was performed using PCA technique, which was effective in maximizing the separation of data samples. Further, multiple linear regression model was formulated to quantify ATCh in the presence of toxicants.

Acknowledgements The authors are grateful to the Department of Science & Technology, New Delhi for their financial support (DST/TM/WTI/2K14/197(a)(G)), (SR/FST/ETI-284/2011 (C)), (SR/FST/LSI-453/2010) and (SR/NM/PG-16/2007). The research was supported by Professor T. R. Rajagopalan research fund, SASTRA University. We also acknowledge SASTRA University, Thanjavur for extending infrastructural support to carry out the study.

References

Alzahrani E, Ahmed RA (2016) Synthesis of copper nanoparticles with various sizes and shapes: application as a superior non-enzymatic sensor and antibacterial agent. Int J Electrochem Sci 11:4712–4723

Bahman E, Shojaosadati SA, Daneshgar P, Norouzi P, Mousavi SM (2011) Performance evaluation of fast fourier transform cyclic-voltammetry pesticide biosensor. Anal Chim Acta 687:168–176

Bucur MP, Bucur B, Radu GL (2013) Critical evaluation of acetylthiocholine iodide andacetylthiocholine chloride as substrates for amperometric biosensors based on acetylcholinesterase. Sensors 13:1603–1613.

Dan D, Huang H, Cai J, Zhang A, Ding J, Chen S (2013) An amperometric acetylthiocholine sensor based on immobilization of acetylcholinesterase on a multiwall carbon nanotube–cross-linked chitosan composite. Anal Bioanal Chem 387:1059–1065

Deng Q, Dong S (1996) Acetylcholinesterase amperometric detection system based on a cobalt(II) tetraphenylporphyrin-modified electrode. The Analyst 121:1123

Ebrahimi B, Shojaosadati SA, Mousavi SM (2010) Evaluation and optimization of factors affecting the performance of a flow-through system based on immobilized acetylcholinesterase as a biosensor. Biotechnol Bioprocess Eng 15:383–391.

Er JK, Ng SH, Li KHH, Shin CS, Su PC, Tay NB, Wang W, Yoon YJ (2014) Detection of thiocholine ions with cobalt phthalocyanine mediated screen printed electrode. Int J Precis Eng Manuf 12:2573–2579

Ivanov Y, Marinov I, Gabrovska K, Dimcheva N, Godjevargova T (2010) Amperometric biosensor based on a site-specific immobilization of acetylcholinesterase via affinity bonds on a nanostructured polymer membrane with integrated multiwall carbon nanotubes. J Mol Catal B Enzym 63:141–148

Kozhushner MA, Trakhtenberg LI, Bodneva VL, Belisheva TV, Landerville AC, Oleynik II (2014) Effect of temperature and nanoparticle size on sensor properties of nanostructured tin dioxide films. J Phys Chem C 118:11440–11444

Marinov I, Ivanov Y, Gabrovska K, Godjevargova T (2010) Amperometric acetylthiocholine sensor based on acetylcholinesterase immobilized on nanostructured polymer membrane containing gold nanoparticles. J Mol Catal B Enzym 62:67–75

Mukherjee J, Lumibao CY, Kirchhoff JR (2009) Application of a thiol-specific electrocatalytic electrode for real-time amperometric monitoring of enzymatic hydrolysis. Analyst 134:582–586

Pandey PC, Singh V (2011) Electrochemical polymerization of aniline over tetracyanoquinodimethane encapsulated ormosil matrix: application in the electrocatalytic oxidation of ascorbic acid and acetylthiocholine. The Analyst 136:1472

Pandey PC, Upadhyay S, Pathak HC, Pandey CMD, Tiwari I, (2000) Acetylthiocholine/acetylcholine and thiocholine/choline electrochemical biosensors/sensors based on an organically modified sol–gel glass enzyme reactor and graphite paste electrode, Sens Actuators B Chem 62:109–116

Quirós MB, Renedo OD, Lomillo MAA, Martínez MJA (2014) Acetylcholinesterase inhibition-based biosensor for aluminum(III) chronoamperometric determination in aqueous media. Sensors 14:8203–8216.

Ramachandra BL, Nesakumar N, Sethuraman S, Krishnan UM, Rayappan JBB (2015) Investigation of electron transfer properties of nanoceria based acetylcholine biosensor using chemometric methods. J Comput Theor Nanosci 12:1–9

Ramnani P, Saucedo NM, Mulchandani A (2016) Carbon nanomaterial-based electrochemical biosensors for label-free sensing of environmental pollutants. Chemosphere 143:85–98

Song Y, Chen J, Sun M et al (2016) A simple electrochemical biosensor based on AuNPs/MPS/Au electrode sensing layer for monitoring carbamate pesticides in real samples. J Hazard Mater 304:103–109

Xie Q, Zhao Y, Guo H, Lu A, Zhang X, Wang L, Chen MS, Peng DL (2013) Facile preparation of well-dispersed CeO_2–ZnO composite hollow microspheres with enhanced catalytic activity for CO oxidation. ACS Appl Mater Interfaces 6:421–428

Zhou N, Li C, Mo R et al (2016) A graphene/enzyme-based electrochemical sensor for sensitive detection of organophosphorus pesticides. Surf Rev Lett 23:1–8